

Electron Collisions with OClO using the R-matrix method

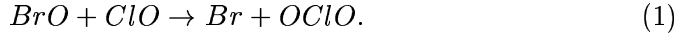
K. L. Baluja[†], N. J. Mason, L. A. Morgan and Jonathan Tennyson,
Department of Physics and Astronomy,
University College London,
Gower Street, London WC1E 6BT, UK
[†] Permanent address:
Department of Physics and Astrophysics,
University of Delhi, Delhi 110007, India

Abstract

The R-matrix method is used to calculate elastic and excitation cross sections of four low-lying electronic states of the OClO molecule, designated the X 2B_1 , 1^2A_1 , 1^2B_2 and 1^2A_2 states. Eight states, four doublets and four quartets, are included in the close-coupled expansion; these excited states are predicted to have vertical excitation energies in the range 2.956 eV to 8.206 eV, in fair agreement with published multireference configuration interaction calculation. The experimentally determined excitation energy of the atmospherically most important state 1^2A_2 centered around 3.5 eV is in excellent agreement with our value of 3.44 eV. A bound state of OClO⁻ with 1A_1 symmetry with an adiabatic electron affinity of 1.558 eV at equilibrium geometry of OClO is found. There is a shape resonance of 3B_1 symmetry at 2.96 eV and higher lying shape resonances of 1B_1 , 1A_2 and 3A_2 symmetries located at 5.75 eV, 8.06 eV and 7.22 eV respectively. All the resonances are rather broad. The resonance positions correlate well with the maxima found in dissociative electron attachment cross section measurements. Rotationally inelastic scattering cross sections are compared with experiment and there is very good agreement for electron energies above 100 meV. Excitation cross sections for three excited states are presented for electron impact energies up to 10 eV. Total integral cross sections are also compared with experiment.

1 Introduction

It is now well established that the depletion of ozone layer occurs during springtime in the stratospheric polar vortex above Antarctica (Cicerone 1987, Rowland 1991). The ozone-destroying reaction cycles involve reactive halogen free radicals whose main sources are chlorofluorocarbons (CFC) and chlorofluorobromocarbons (halons). An important ozone loss cycle involves the coupling of chlorine and bromine chemistry in the upper atmosphere in which OClO plays a key role. The OClO molecule is stratospherically important due to its abundance during polar nights. It is formed by the bimolecular reaction:



OClO is therefore used as an indicator for monitoring the stratospheric bromine budget.

Although the spectroscopy of OClO has been extensively studied, the interaction of electrons with OClO molecule remains poorly characterized. In previous studies, we reported the first data on electron-impact scattering from ClO molecule (Baluja *et al.* 2000) and from Cl₂O molecule (Baluja *et al.* 2001). This data was generated using the R-matrix method employing the UK polyatomic R-matrix code (Morgan *et al.* 1997, 1998). In the present paper, we extend this study to OClO molecule.

Experimental work on OClO is difficult because it is explosive and inherently unstable, and must be handled with caution. The optical absorption of OClO has been studied extensively. For example Wahner *et al.* (1987) and Hubinger and Nee (1994) recorded the absorption spectrum in the energy range 2.5–4.4 eV where the photoabsorption cross section is dominated by the transition from the ground state X ²B₁ to the excited state A ²A₂. These optical absorption measurements were subsequently extended up to 12.5 eV using synchrotron electron energy-loss spectroscopy (Davies *et al.* 1995). Electron impact experiments include the study of dissociative electron attachment of Marston *et al.* (1998) and Senn *et al.* (1999) for electron energies up to 10 eV. These experiments revealed the presence of collision thresholds which maybe ascribed to either shape or Feshbach resonances which were apparent at about 0, 0.7, 4.3, 6 and 8 eV.

Total cross sections for the scattering of electrons from OClO have been reported by Gulley *et al.* (1998) in the electron energy range from 9 meV to 10 eV. At very low energies, their cross sections show structure probably due to rotationally inelastic scattering. There was a sharp minimum in the cross section at 38 meV and a subsequent maximum at electron impact energies between 55 and 60 meV. These results also indicate a broad shoulder between 2 and 6 eV. However the experiments of Gulley *et al.* were later found to contain a strong residual due to the contaminant Cl₂, hence these cross sections were re-measured by Field *et al.* (2000) with a purity level of OClO exceeding 90 %.

The new cross sections are significantly larger than the previous results. Cross sections for backward scattering of electrons from OClO were also reported in the range 20–500 meV. The ratio of backward to the integral cross section is a qualitative measure of the efficiency of electron attachment. The backward scattering data indicates that dissociative attachment at low energies occurs through p-wave attachment. Other electron collision studies involving electron impact ionization (O'Connor *et al* 1998, Muigg *et al* 2001) have been reported recently.

The open shell nature of many of the Cl_xO_y compounds make them difficult systems to treat theoretically. Electron correlation plays an important role in these systems, not only for characterizing the ground state wavefunction, but also the many low-lying excited states which significantly affect low energy electron collisions. Since OClO is an open shell system, electron correlation plays a dominant role in determining the transition energies and transition moments among various electronic states.

In this paper we report the first electron collision calculations on OClO. These calculations are performed using the UK polyatomic R-matrix code (Morgan *et al* 1997, 1998), taking particular advantage of this method to give a good representation of the electron correlation in several excited states of the molecule (Tennyson 1996a).

2 Method

2.1 General considerations

The R-matrix method (Burke and Berrington 1993) divides configuration space into two regions. In the inner region, here defined by a sphere of radius 10 a₀ centered at the OClO centre of mass, the wavefunction is written using the configuration interaction (CI) expression:

$$\Psi_k = \mathcal{A} \sum_{ij} a_{ijk} \phi_i^N \eta_{ij} + \sum_j b_{jk} \phi_j^{N+1} \quad (2)$$

where ϕ_i^N represents the *i*th state of the N-electron target, η_{ij} is a function representing the continuum electron and \mathcal{A} an anti-symmetrisation operator. The continuum functions are the only functions with amplitude on the R-matrix boundary. The second sum in (1) comprises configurations composed of short-range functions. To obtain reliable results it is important to maintain a balance between the N-electron target representation, ϕ_i^N , and the N+1 electron scattering wavefunction. The choice of appropriate ϕ_j^{N+1} is crucial in this (Tennyson 1996b). Coefficients a_{ijk} and b_{jk} are variational parameters determined as a result of the matrix diagonalisation.

Inside the R-matrix sphere full electron-electron and exchange interactions are explicitly modelled. Outside the sphere, only long-range multipolar

interactions between the scattering electron and the various target states are included. OClO is a strongly dipolar system which has to be taken into account both by propagating the R-matrix to large distance, $50 a_0$ in the present work, and by considering convergence with respect to the partial wave expansion used for the continuum orbitals, η_{ij} .

2.2 Target states

The equilibrium structure of OClO was determined by Flesch *et al* (1993). OClO molecule is bent and belongs to the C_{2v} symmetry group. At the equilibrium geometry, the Cl-O bond length is 1.471 Å and the angle OClO is 117.5° . These parameters are used in the present calculations.

The OClO molecule is rich in electrons. Its electronic ground state configuration has been established through optical absorption study (Peterson and Werner 1992, Flesch *et al* 1993). There are 14 core electrons and 19 valence electrons. The core consists of doubly occupied $1a_1$, $2a_1$, $3a_1$, $4a_1$, $1b_1$, $1b_2$ and $2b_2$ molecular orbitals. The 19 valence electrons are distributed in 10 molecular orbitals of type $5a_1$, $3b_2$, $6a_1$, $7a_1$, $4b_2$, $2b_1$, $5b_2$, $8a_1$, $1a_2$ and $3b_1$. For the ground state all molecular orbitals upto $1a_2$ are doubly occupied giving the state designation X^2B_1 . The first three electronic excited states are formed in which one of the electron from the molecular orbitals $1a_2$, $8a_1$ or $5b_2$ is promoted to $3b_1$ molecular orbital yielding the state designations 1^2A_2 , 1^2A_1 and 1^2B_2 respectively for the three lowest electronic excited states. Of these, state 1^2A_2 is the atmospherically most important. Its excitation gives rise to an intense UV/visible band around 3.5 eV (Peterson and Werner 1992). The state 1^2A_1 has a low oscillator strength and is possibly masked by 1^2A_2 in the absorption spectrum.

Previous theoretical work on the OClO spectrum include a restricted Hartree-Fock calculation (RHF) (Gole 1980) and a multireference configuration interaction (MRCI) calculation (Peterson and Werner 1992) of its four low-lying electronic states. In the MRCI calculation (Peterson and Werner 1992) for the four lowest electronic states, the one-particle basis set employed was the standard correlation consistent polarized quadruple zeta sets of Dunning (1989) for oxygen and a primitive set of Partridge (1987) augmented with a 3d2f polarization set for chlorine. The MRCI calculations were extended (Peterson and Werner 1996) to investigate the potential energy surfaces involved in the photodissociation of OClO to Cl+O₂.

Our calculations on OClO used the double zeta plus polarisation Gaussian basis sets of Dunning and Hay (1977), and Magnusson and Schaefer (1985). We used the the SCF molecular orbitals of the ground state in our configuration interaction calculations of all the four states which are included in the scattering calculation. In our target state calculations, in addition to the 7 core orbitals three more molecular orbitals $5a_1$, $6a_1$ and $3b_2$ were also frozen

in their SCF orbitals. The reduced active space did not make any significant changes to the total energies of the target states. In all our calculations we have employed this model which comprises 20 frozen electrons and 13 valence electrons distributed according to $(7a_1, 8a_1, 9a_1, 2b_1, 3b_1, 4b_2, 5b_2, 6b_2, 1a_2)^{13}$. We refer to this model as a complete active space configuration interaction (CASCI) model. Our SCF calculations indicate that the highest occupied molecular orbital is $3b_1$ with a binding energy of -6.14 eV. The lowest unoccupied molecular orbital is $9a_1$ with energy $+4.72$ eV and the next unoccupied orbital is $6b_2$ with energy $+5.36$ eV. All the three excited electronic states included in our calculations arise due to the promotion of one electron from one of the three valence molecular orbitals $5b_2$, $8a_1$ and $1a_2$ to the already singly occupied molecular orbital $3b_1$. Table 1 presents vertical excitation energies for the states considered in our calculation. These are in good agreement with the calculations of (Peterson and Werner 1992). The experimentally determined excitation energy of the atmospherically most important state 1^2A_2 centered around 3.5 eV band is in excellent agreement with our value of 3.44 eV.

Our CASCI model gives a dipole moment of 2.293 D and quadrupole moments $Q_{20} = -1.755$ au and $Q_{22} = -3.898$ au at the equilibrium geometry of OCIO molecule. This value of dipole moment is in reasonable agreement with the value 2.084 D calculated by McGrath *et al* (1990) who used a polarized split-valence basis set using second-order Moller-Plesset (MP2) perturbation theory. The difference of about ten percent between two theoretical values is due to different basis sets, different amount of correlation, and a slight difference in the equilibrium geometries involved. These theoretical values are higher than the two measured values of the dipole moment of OCIO by Tolles *et al* (1962) using Stark effect with a value 1.784 D, and by Tanaka and Tanaka (1983) using laser Stark spectroscopy with a value of 1.792 D.

2.3 Scattering Model

Our best model used the eight target states given in Table 1 in the close-coupling expansion (1). We also performed test scattering calculations in the static-exchange (SE) and static-exchange with polarization (SEP) models. All calculations were performed for singlet and triplet states with A_1 , B_1 , B_2 and A_2 symmetries. In these calculations, the continuum orbitals were represented by Gaussians centered at the molecule centre of gravity. For this the orbitals of Sarpal *et al* (1996) were used. All calculations were performed for continuum orbitals up to f ($l \leq 3$). These continuum orbitals were orthogonalized to the target orbitals retained in the calculation and those with an overlap of less than 2×10^{-7} were removed (Morgan *et al* 1997).

Calculations, from SE upwards, were performed to test the stability of our model and assign resonances. These calculations included some with hand

picked configurations which allowed us to give orbital designations to the resonances we found and to probe the cause of pseudo-resonances which are high energy artifacts of any truncated coupled channels calculation.

One advantage of the CAS CI target model employed here is that the ϕ_j^{N+1} functions, see (1), can be defined in a fashion which retains the balance of the calculation (Tennyson 1996b). All $N + 1$ electron configurations of the appropriate total symmetry given by (core)²⁰ ($7a_1, 8a_1, 9a_1, 2b_1, 3b_1, 4b_2, 5b_2, 6b_2, 1a_2$)¹⁴ were retained. This means that 20 electrons are frozen in the core and 14 electrons are free to move among the molecular orbitals as given within the bracket.

3 Results

3.1 Anionic Bound State

Our CI model gives a value of 2.293 D for the dipole moment of OCIO which is strong enough to support a bound state of the anion. All the scattering models except SE model found a bound state of OCIO with 1A_1 symmetry. The energy of state was determined using our bound state detecting code BOUND (Sarpal *et al* 1991). Our best model gave OCIO an electron affinity of 1.547 eV at its equilibrium geometry. The inclusion of rotational motion (Crawford and Garrett 1977) will reduce the anionic binding energy but the strong dipolar nature of OCIO will keep the anionic state intact.

We also performed a standard bound state quantum chemistry calculation on the anionic state of 1A_1 symmetry using the same orbitals and model employed for the scattering calculations. This calculation gave a very similar result, an OCIO electron affinity of 1.558 eV at the equilibrium geometry. From photoelectron spectroscopy (Gilles *et al* 1992) the adiabatic electron affinity of OCIO is 2.14 eV. Given the difference between vertical and adiabatic binding energies these results are consistent with each other. However we note that our SEP model only yields a weak anionic binding energy of 0.52 eV.

3.2 Elastic scattering

We carried out the scattering calculations in four models. These are SE, SEP, 4-state and 8-state models. Our best model is the 8-state model. In this model, 16 channels are coupled for singlet scattering symmetries and 32 channels for triplet symmetries. The number of configuration state functions for each triplet and singlet scattering symmetry is around 5900 and 3900 respectively. Due to the presence of long range dipole interaction, the elastic cross section is formally divergent in the fixed-nuclei approximation. However, the elastic scattering data can be exploited to yield rotationally summed cross sections. Due to the permanent nature of dipole moment of OCIO molecule, a very

large number of partial waves must be taken into account to obtain converged results. States with ($l \geq 4$) omitted from our calculations were allowed for by using the Born approximation (Gianturco and Jain 1986). The rotational spectrum of OClO has been analyzed in great detail by Muller *et al* (1997). The rotational constants for OClO at the equilibrium geometry are 1.73724 cm^{-1} , 0.33198 cm^{-1} , and 0.27800 cm^{-1} (Muller *et al* 1997). OClO molecule is an asymmetric top but has one moment of inertia considerably greater than either of the other two. The value of the asymmetry parameter is -0.926 , which is close to -1 , and therefore to a good approximation it may be treated as a prolate symmetric top.

Figure 1 presents integral rotationally inelastic scattering cross sections for our 8-state model and compare these with the experiment (Field *et al* 2000) for electron energies up to 500 meV. Since low-energy scattering of electrons from polar molecules is largely determined by electron-permanent-dipole interaction, we have used the experimental value 1.792 D (Tanaka and Tanaka 1983) in the outer region. Use of the larger theoretical dipole moment in the outer region gives slightly higher cross sections for energies up to 300 meV, above which there is hardly any difference. Fig. 1 also shows the contribution of summed singlet and summed triplet scattering symmetries up to f partial waves. Our Born-corrected cross sections are in good agreement with the experimental values at energies above 100 meV, but do not reproduce the sharp minimum observed in the cross section below this. If this minimum is due to interference effects between rotational excitation and other channels, as suggested by Field *et al*, then it could only be modelled by a more sophisticated treatment of the rotational excitation problem than we employ here.

The main feature in the elastic cross section is the presence of resonances in the 1B_1 , 3B_1 , 1A_2 and 3A_2 symmetries. In figure 2, we present cross sections for the 3B_1 resonance in the 4-state and 8-state models. For the 8-state model the 3B_1 feature is a shape resonance is located at 2.961 eV with a width 0.843 eV. For the 4-state model, this resonance lies at higher energy of 4.011 eV, ie above the doublet excited states. As the number of states included in the calculation increase, the position of the resonance shift to a lower energy and becomes narrower. This is due to the increased attractive polarization potential experienced by the scattering electron.

The 1B_1 resonance in the 8-state model is located at 5.750 eV with a width 1.405 eV. For the 4-state model this resonance position moves to a higher energy at 5.843 eV and is even broader than the 8-state result. The 3A_2 resonance in the 8-state model is located at 7.22 eV with a width 1.50 eV, while the corresponding values for the 1A_2 resonance are 8.06 eV and 2.72 eV. These broad resonance features are present even in the SE model, provided we use a complete active space CI target wavefunction, and therefore are probably best described as a shape resonances. Our previous study on Cl_2O^- (Baluja *et al* 2001) also found a number of shape resonances which therefore seem to

be a particular feature of these electron rich oxides of chlorine.

The dominant configuration of 1B_1 and 3B_1 resonances is $3b_19a_1$; it should be noted that the $9a_1$ orbital is substantially of p character. The dominant configuration of 1A_2 and 3A_2 shape resonances is $3b_16b_2$. The resonant positions at 5.750 eV and 2.961 eV correlate approximately with maxima in the cross sections in the dissociative electron attachment observed by Marston *et al* (1998) and Senn *et al* (1999), which lie near 6 eV and 4.3 eV respectively.

3.3 Inelastic cross sections

Figures 3, 4 and 5 present OClO electron impact electronic excitation cross sections from the ground state to the doublet excited states included in the calculations. According to the symmetry group and the optical selection rules, transitions from the ground state to all doublet excited states are dipole allowed except those to the 2B_2 state.

The first excited state has symmetry 2B_2 . The corresponding integrated cross sections are shown in Fig.3 for our 4-state and 8-state calculations. The contribution of singlet and triplet symmetries for our best model are shown. The most significant contribution comes from 1A_1 symmetry and the next important contribution is from 1B_2 symmetry. The contribution from 1A_2 and 1B_1 symmetries is almost negligible. The triplet symmetries 3B_2 and 3A_1 dominate over the remaining triplets. For this optically forbidden transition, the total contribution from the singlet symmetries is much more than the total contribution from the triplet symmetries. The summed triplet cross section is almost flat over the entire energy range. In contrast, the summed singlet cross sections show a peak in the cross section at 8 eV which is due to combined effect of 1B_2 and 3B_2 symmetries. The cross-sections in our best model are lower in magnitude than our 4-state model due to the loss of flux into other accessible channels. The peak around 8 eV is shifted to a slightly higher energy when the quartet states are excluded from the scattering calculation.

The cross section for exciting the second, 2A_1 , state is shown in figure 4. This is a dipole allowed transition but is weak with a transition moment of 0.0821 au. The 2B_2 and 2A_1 states are almost degenerate but the integrated cross sections for exciting the 2A_1 state are higher than the excitation of 2B_2 state due to the former state being optically allowed. We have shown the contribution of singlet and triplet symmetries for our best model. The triplet contribution is more than the corresponding contribution from singlets up to 9 eV. Among the singlets, the 1A_1 symmetry is dominant. The 1B_2 symmetry begins to contribute beyond 8 eV, the remaining singlets have negligible effect on the cross section. The cross section due to 3A_1 symmetry rises sharply at the threshold and has a peak around 6.5 eV. There is also a peak in the cross section in the 3B_2 symmetry at about 8 eV. The net effect of all the singlets and triplet symmetries is to produce a hump around 8 eV. The cross sections

for our 8-state model are lower than the 4-state results above the threshold of the first excited quartet state.

In figure 5, we have displayed the cross sections for the excitation of 2A_2 state. This is a dipole allowed transition with a transition moment of 0.6092 au. The structure in the 4-state and 8-state models arises in the 3A_2 symmetry. The peak in the best model is shifted by almost 1 eV when quartets are included in the scattering calculation with respect to 4-state model which only includes doublet target states. To obtain converged cross sections, the contribution of partial waves higher than f-wave have been accounted for through closure relations (Crawford and Dalgarno 1971) in the Born approximation. The uncorrected and Born-corrected cross sections for our 8-state model are shown. Away from threshold, the contribution of higher partial waves are quite important for this strong dipole allowed transition. The cross section due to singlets rises from threshold and then becomes almost constant beyond 4 eV. The cross section due to 3A_2 symmetry is very prominent and contributes almost half to the integrated cross section at the peak. All the remaining triplets contribute significantly. Among the singlets, the contribution of 1A_2 symmetry is almost half to the summed cross section for singlets.

Finally, in figure 6 we present total (elastic plus excitation) cross sections for the 8-state model and compare these with the (rescaled) experimental data of Gulley *et al* (1998). Due to the presence of an impurity in the OCIO sample, the measured values for total scattering cross sections were found to be too low. Therefore we have renormalized the data to the new, high purity values of Field *et al* (2000) at 0.5 eV. The result is good agreement between both the magnitude and shape of the theoretical and experimental results. In particular we note that our calculations reproduce the broad shoulder between 2 eV and 6 eV in the experimental results.

4 Conclusions

This is the first theoretical study of electron impact on open-shell radical OCIO. Our calculations predict a bound anionic state and four shape resonances which correlate with maxima observed in the dissociative electron attachment cross sections. Our calculations also agree quantitatively with the total cross sections in the several hundred meV range and reproduce the salient features like the presence of a shoulder in the few eV range. This is encouraging and suggests that the results reported by us previously on ClO (Baluja *et al* 2000) and Cl₂O (Baluja *et al* 2001), for which there was no experimental data available for comparison, should provide accurate predictions above the low-energy region. However our calculations do not reproduce the sharp minima observed in the cross section at electron energies below 100 meV; such behaviour can probably only be modelled with a much more sophisticated

treatment of the electron impact rotational excitation problem than the one used here.

Acknowledgments

This work was supported by the UK Engineering and Physical Sciences Research Council via a visiting Fellowship for KLB and other grants.

References

- Baluja K L, Mason N J, Morgan L A and Tennyson J 2000 *J. Phys. B: At. Mol. Opt. Phys.* **33** L677
- 2001 *J. Phys. B: At. Mol. Opt. Phys.* in press
- Burke P G and Berrington K A (eds) 1993 Atomic and molecular Processes: an R-matrix approach 1993 (Institute of Physics Publishing, Bristol and Philadelphia)
- Cicerone R J 1987 *Science* **237** 35
- Crawford O H and Garrett W R 1977 *J. Chem. Phys.* **66** 4968
- Crawford O H and Dalgarno A 1971 *J. Phys. B: At. Mol.* **13** 494
- Davies J A, Mason N J, Marston G and Wayne R P 1995 *J. Phys. B: At. Mol. Opt. Phys.* **28** 4179
- Dunning T H and Hay P J 1977 in Methods of Electronic Structure Theory, vol. 2 (Plenum, New York) (Edited by H F Schaefer)
- Dunning T H 1989 *J.Chem.Phys.* **90** 1007
- Field D, Jones N C, Gingell J M, Mason N J, Hunt S L and Ziesel J P 2000 *J. Phys. B: At. Mol. Phys* **33** 1039
- Flesch R, Ruhl E, Hottmann K and Baumgartel H 1993 *J. Phys. Chem.* **97** 837
- Gianturco F A and Jain A 1986 *Physics Reports* **143** 347
- Gilles M K, Pollak M L and Lineberger W C 1992 *J. Chem. Phys.* **96** 8012
- Gole J L 1980 *J.Phys.Chem.* **84** 1333
- Gulley R J, Field T A, Steer W A, Mason N J, Lunt S L, Ziesel J P and Field D 1998 *J. Phys. B: At. Mol. Opt. Phys.* **31** 5197
- Hubinger S and Nee J B 1994 *Chem. Phys.* **181** 247
- Magnusson E and Schaefer H F 1985 *J. Chem. Phys.* **83** 5721
- Marston G, Walker I C, Mason N J, Gingell J M, Zhao H, Brown K L, Motte-Tollet F, Delwiche J and Siggel M R F 1998 *J. Phys. B: At. Mol. Opt. Phys.* **31** 3387
- McGrath M P, Clemitchaw K C, Rowland F S and Hehre W J 1990 *J. Phys. Chem.* **94** 6126
- Meincke M, Schmale C, Ruehl E and Illenberger E 1991 17th Int. Conf. on Physics of Electronic and Atomic Collisions (Australia: Brisbane) Abstracts p 262
- Morgan L A, Gillan C J, Tennyson J and Chen X 1997 *J. Phys. B: At. Mol. Opt. Phys.* **30** 4087
- Morgan, L A, Tennyson J and Gillan C J 1998 *Computer Phys. Commun.* **114** 120
- Muigg D, Denifel G, Stamatovic A, Mason N J and Mark T D 2001 *J. Chem. Phys.* in press

- Muller H S P, Sorensen G O, Birk M and Friedl R R 1997 *J.Mol.Spectrosc.* **186** 177
- O'Connor C, Tafadar T and Price S D 1998 *J. Chem. Soc. Faraday Trans.* **94** 1797
- Partridge H R 1987 Nasa Technical Memorandum 89449
- Peterson K A and Werner H J 1992 *J. Chem.Phys.* **96** 8948
- 1996 *J. Chem.Phys.* **105** 9823
- Rowland F S 1991 *Annu. Rev. Phys. Chem.* **42** 731
- Sarpal B K, Branchett S E, Tennyson J and Morgan L A 1991 *J. Phys. B: At. Mol. Opt. Phys.* **24** 3685
- Sarpal B K, Pfingst K, Nestmann B M and Peyerimhoff S D 1996 *J. Phys. B: At. Mol. Opt. Phys.* **29** 857
- Senn G, Drexel H, Marston G, Mason N J, Mark T D, Meinke M, Schamle C, Tageder P, Ruhl E and Illenberger E 1999 *J. Phys. B.* **32** 3615
- Tanaka K and Tanaka T 1983 *J.Mol.Spectrosc.* **98** 425
- Tennyson J 1996a *J. Phys. B: At. Mol. Opt. Phys.* **29** 1817
- 1996b *J. Phys. B: At. Mol. Opt. Phys.* **29** 6185
- Tolles W M, Kinsey J L, Curl Jr R F and Heidelberg R F 1962 *J. Chem. Phys.* ?? 927
- Wahner A, Tyndall G S and Ravishankara A R 1987 *J. Phys. Chem.* **91** 2734

Table 1: Vertical energy excitations (in eV) for the OCIO target states generated using a CASCI model at the experimental geometry of the ground state. Also given are the dominant configuration of each state, the number of configurations, N , in the CAS and the theoretical values of Peterson and Werner(1992).

| State | Configuration | N | Vertical excitation energies | |
|-----------|-----------------------|-----|------------------------------|---------------------------|
| | | | This work | Peterson and Werner(1992) |
| X 2B_1 | | 473 | 0 | |
| 1 2A_1 | $8a_1^{-1} 3b_1^2$ | 477 | 2.96 | 3.15 |
| 1 2B_2 | $5b_2^{-1} 3b_1^2$ | 477 | 2.99 | 3.20 |
| 1 2A_2 | $1a_2^{-1} 3b_1^2$ | 463 | 3.44 | 3.66 |
| 1 4B_2 | $1a_2^{-1} 3b_1 9a_1$ | 258 | 6.52 | 6.82 |
| 1 4A_2 | $6b_2 3b_1 9a_1$ | 246 | 6.87 | 7.96 |
| 1 4A_1 | $5b_2^{-1} 3b_1 9a_1$ | 246 | 7.03 | 8.08 |
| 1 4B_1 | $8a_1^{-1} 3b_1 9a_1$ | 258 | 8.21 | 8.27 |

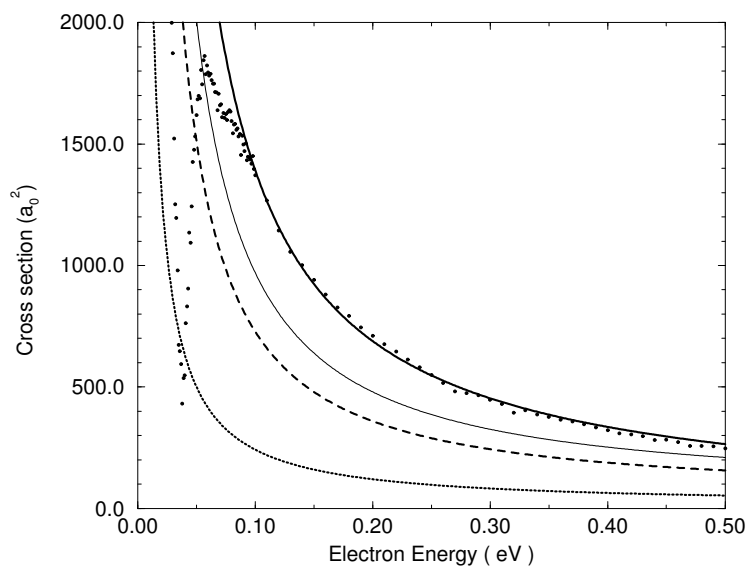


Figure 1: 8-state R-matrix elastic (up to f partial wave) and rotational cross sections for electron impact on X 2B_1 state of OClO Dotted line (singlet symmetries, elastic cross sections); Dashed line (triplet symmetries, elastic cross sections); Thin solid line (singlet+triplet symmetries, elastic cross sections); Solid line (Born-corrected summed rotational cross section); dots (Experiment, Field *et al* 2000)

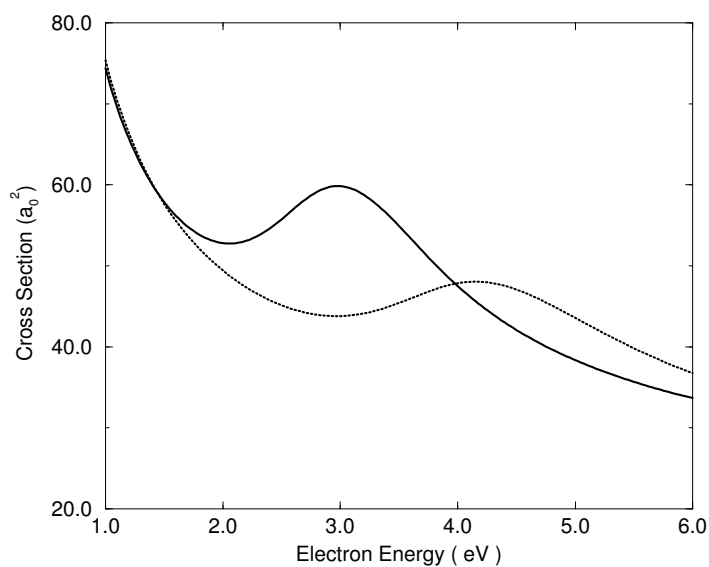


Figure 2: 3B_1 contribution to the total cross section including Born correction illustrating the role of the 3B_1 shape resonance: Solid line (8-state R-matrix); Dotted line (4-state R-matrix);

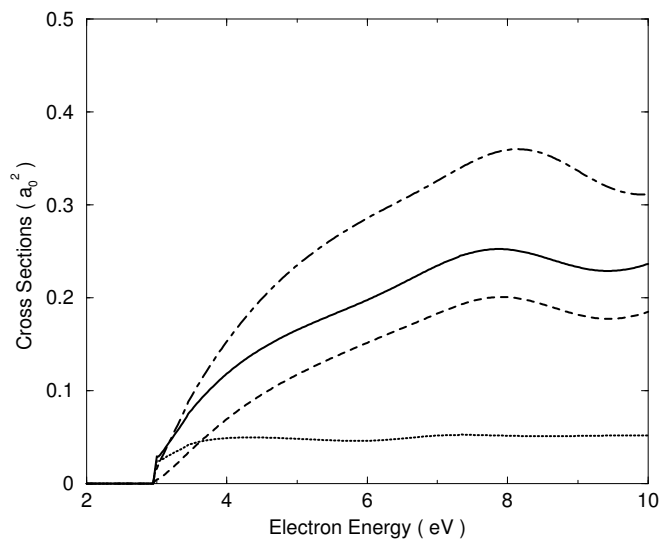


Figure 3: Electron impact excitation of transition $X \ ^2B_1-1 \ ^2B_2$ of OCIO. Solid line (8-state R-matrix cross sections); Dash-dotted line (4-state R-matrix cross sections); Dotted line (8-state R-matrix cross sections for triplet symmetries); Dashed line (8-state R-matrix cross sections for singlet symmetries)

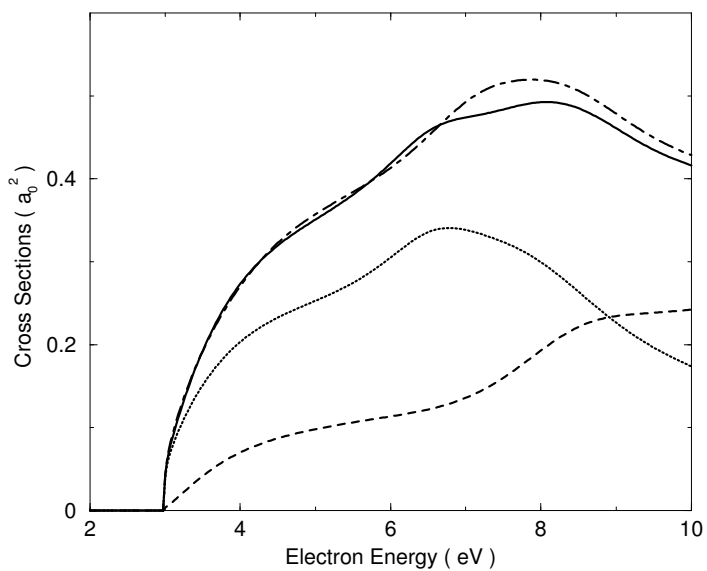


Figure 4: Electron impact excitation of transition $X \ ^2B_1-1 \ ^2A_1$ of OCIO. Solid line (8-state R-matrix cross sections); Dash-dotted line (4-state R-matrix cross sections); Dotted line (8-state R-matrix cross sections for triplet symmetries); Dashed line (8-state R-matrix cross sections for singlet symmetries)

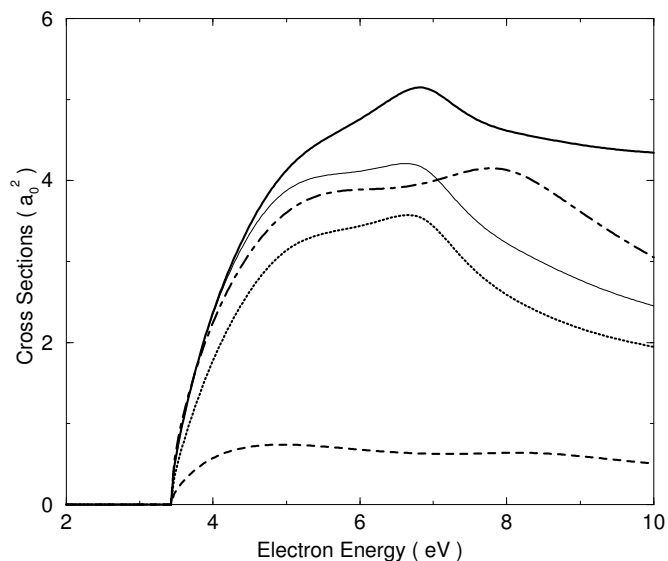


Figure 5: Electron impact excitation of transition $X \ ^2B_1-1 \ ^2A_2$ of OCIO. Solid line (Born-corrected 8-state R-matrix cross sections); Thin solid line (Uncorrected 8-state R-matrix cross sections); Dash-Dotted line (4-state R-matrix cross sections); Dotted line (8-state R-matrix cross sections for triplet symmetries); Dashed line (8-state R-matrix cross sections for singlet symmetries)

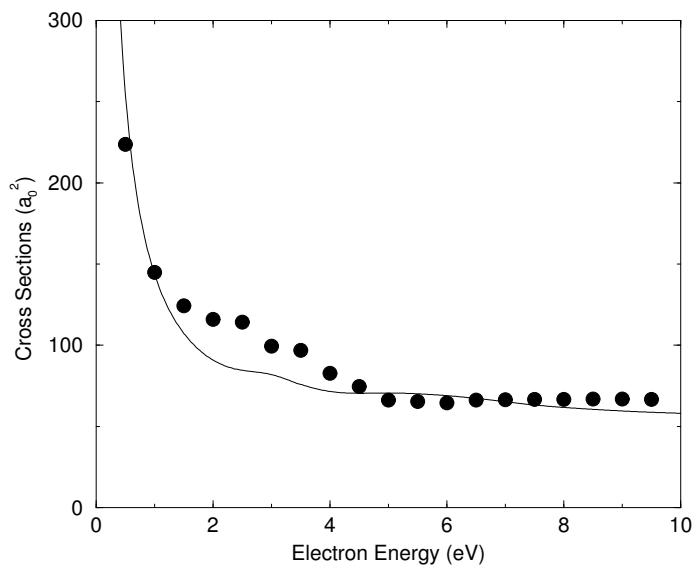


Figure 6: Total (elastic+excitation) cross section for electron impact of OCIO. Solid line: 8-state R-matrix cross sections; Circles: rescaled experiment of Gulley *et al* (1998), see text for details.